Journal of the European Ceramic Society 22 (2002) 2013–2021

www.elsevier.com/locate/jeurceramsoc

Effect of preparation conditions on cation ordering and dielectric properties of $Ba(Mg_{1/3}Ta_{2/3})O_3$ ceramics

T.V. Kolodiazhnyi[a], A. Petric[a,*], G.P. Johari[a], A.G. Belous[b]

[a]*Department of Materials Science and Engineering, McMaster University, Hamilton, Ontario, L8S 4L7, Canada*
[b]*Institute of General and Inorganic Chemistry, 32/34, Palladina Ave., Kyiv-142, Ukraine*

Received 1 August 2001; received in revised form 2 November 2001; accepted 17 November 2001

Abstract

The effect of preparation conditions on cation ordering and dielectric properties of $Ba(Mg_{1/3}Ta_{2/3})O_3$ ceramics was investigated. Preparation of $Ba(Mg_{1/3}Ta_{2/3})O_3$ by conventional synthesis from $BaCO_3$, MgO, and Ta_2O_5 was compared to an alternate route of reaction of $MgTa_2O_6$ with $BaCO_3$. It was shown that in the conventional synthesis method, intermediate phases inhibit formation of single-phase $Ba(Mg_{1/3}Ta_{2/3})O_3$ up to 1400 °C, whereas utilization of a $MgTa_2O_6$ precursor produces the nearly pure perovskite phase after heat treatment at 1000 °C. In the temperature range of 1400–1620 °C, the $Ba(Mg_{1/3}Ta_{2/3})O_3$ ceramic remains single phase. Traces of the $Ba_3Ta_5O_{15}$ phase were detected by XRD and EDX in samples sintered above 1630 °C. Decrease in the 1:2 cation ordering and increase of dielectric loss were observed in samples sintered at $T > 1590$ °C.

Keywords: $Ba(Mg,Ta)O_3$; Dielectric properties; Ordering; Perovskites; Phase development

1. Introduction

The dielectric ceramic, $Ba(Mg_{1/3}Ta_{2/3})O_3$ or BMT, has found wide application in X (8–12 GHz), Ku (12–18 GHz), and K (18–27 GHz) frequency bands. Owing to its exceptionally low dielectric loss (high Q-factor) and temperature stable coefficient of resonance frequency, it has been utilized as a dielectric resonator in output multiplexers of communication satellites.[1] This has considerably decreased insertion losses and hence increased the output microwave power of the satellite. BMT-based dielectric resonators have also been used in microwave oscillators, base stations, radar detectors, etc.

Obtaining BMT ceramic with a high Q-factor is a technologically challenging task. BMT with its melting temperature of ca. 3000 °C,[2] is considered one of the most refractory oxides. Several papers have addressed the preparation of high Q BMT ceramics.[3–6] Nomura et al.[3] obtained high-density (98%) BMT with $Q \times f = 168$ THz by doping with 1 mol% of Mn. Matsumoto et al.[4] found that fast heating rates of up to 500 °C/min produce BMT ceramics with $Q \times f = 400$ THz. Another group, Matsumoto et al.,[5] obtained BMT of $Q \times f = 430$ THz after sintering for 20 h at 1640 °C. The latter group has also claimed that $BaSnO_3$ is an effective dopant for tuning the temperature coefficient of the resonance frequency, τ_f, in the range of −0.5 to +5.4 ppm/°C.

It is considered that both the high density of the ceramic and the high degree of 1:2 ordering of B-site cations are responsible for low dielectric loss of BMT at microwave frequencies. Although densification of ceramics increases with sintering temperature, the 1:2 ordered phase remains thermodynamically stable below a certain temperature, T_c, and becomes disordered above this temperature. Until now, however, neither the temperature T_c nor the mechanism of the order–disorder phase transition in BMT has been known unambiguously. Several recent papers have reported a theoretical analysis of a high temperature order-disorder transition in $A(B'_{1/3}B''_{2/3})O_3$ perovskite compounds.[7,8] Takahashi et al.[9] used first-principles calculations to predict that the order–disorder transition in BMT should occur at $T_c = 3500$ °C which is above the melting point. In view of this high value of apparent T_c, the authors[9] proposed that it is beneficial to sinter BMT at

* Corresponding author.
E-mail address: petric@mcmaster.ca (A. Petric).

0955-2219/02/$ - see front matter
PII: S0955-2219(01)00515-5

higher temperatures and longer times to increase the degree of cation ordering. In contrast to this prediction, Guo et al.[2] obtained completely disordered BMT single crystals grown by the laser heated pedestal technique at 2960–3100 °C. Annealing of these crystals at 1600 °C for 3 h did not result in increase in the degree of ordering. While analyzing cation ordering transformations in $Ba(Mg_{1/3}Ta_{2/3})O_3$–$BaZrO_3$ perovskite solid solutions, Chai et al.[10] reported that in pure BMT the 1:2 ordered phase remained stable up to 1650 °C. The sintering temperatures of the BMT ceramics range from 1400 to 1650 °C. However, no detailed analysis of the effect of the sintering temperature on the dielectric properties of BMT has been published so far. Hence the purpose of this paper was to study the effect of preparation conditions on the degree of 1:2 ordering and its subsequent effect on dielectric properties of BMT ceramics.

2. Experimental procedure

In order to investigate the role of precursors, BMT was prepared by two different solid state methods. The first one was a conventional method (referred to as method I) which can be described by the reaction:

$$3BaCO_3 + MgO + Ta_2O_5 \rightarrow 3Ba(Mg_{1/3}Ta_{2/3})O_3 + 3CO_2$$

In the second method (method II) a $MgTa_2O_6$ precursor was prepared first and then reacted with $BaCO_3$, according to:

$$3BaCO_3 + MgTa_2O_6 \rightarrow 3Ba(Mg_{1/3}Ta_{2/3})O_3 + 3CO_2$$

The choice of method II was dictated by its successful application in preparation of $Pb(Mg_{1/3}Nb_{2/3})O_3$[11] and $Ba(Zn_{1/3}Ta_{2/3})O_3$[12] ceramics. High purity (>99.9%) metal oxides and carbonates (MgO, Ta_2O_5, $BaCO_3$ Cerac) were used for both methods. For method II, $MgTa_2O_6$ precursor was prepared by heating MgO and Ta_2O_5 at 1300 °C for 10 h. Stoichiometric amounts of the required powders were milled for 2 h in a Nalgene bottle with ethanol and zirconia grinding balls. The dried powders were pressed into pellets and calcined at 800–1400 °C for 2–10 h. For preparation of ceramic samples, the powders calcined at 1400 °C were ground and vibromilled for 10 h. After addition of a small amount of polyvinyl alcohol binder, the powders were uniaxially pressed into pellets at 800 kg/cm^2 pressure. The pellets were sintered in air at a temperature range between 1550 and 1650 °C for 20 h. The heating and cooling rates were varied from 15 to 200 °C/h.

Phase identification was performed on Rigaku Geigerflex Dmax II diffractometer with CoK_α radiation source ($\lambda = 1.7889$ Å), a step size of 0.02° and a count time of 4 s/step. The microstructure of polished samples was studied by SEM (Philips 515) and optical microscopy (Leitz Wetzlar). Thermally etched samples were analyzed by SEM equipped with EDX (Link Analytical). Samples for TEM (Philips CM12, 120 keV) and electron diffraction were prepared by mechanical grinding followed by dimpling and ion-beam milling until perforation.

Dielectric characterization of the samples in the X-frequency band was performed with an HP 8510 vector network analyzer. Owing to difficulties in determining the Q-factor by the Hakki and Coleman post-resonator technique, as discussed in Ref. 13, a simpler and more reliable transmission method[14] was employed in this work. For transmission measurements, a cylindrical dielectric resonator (DR) shaped into $TE_{01\delta}$ resonant mode was centered in the X-band rectangular copper waveguide using a styrofoam holder. In this configuration, the waveguide serves as a band-stop filter at the $TE_{01\delta}$ resonance frequency. To separate the $TE_{01\delta}$ mode from the higher resonance modes, the samples must have an aspect ratio close to 0.45. The diameter and thickness of the samples was 6 and 2.7 mm, respectively. The unloaded Q-factor was calculated according to:

$$Q = \frac{Q_L}{1 - 10^{-P/20}} \quad (1)$$

where Q_L is the loaded quality factor determined from the full width of the resonance peak at the 3 dB level, and P is the depth of the resonance peak in decibels. As has been pointed out by Zurmühlen et al.,[13] the rectangular waveguide transmission method gives the same values of Q-factor as the commercially utilized cylindrical cavity method.15 However, due to the closer proximity of the sample to the waveguide walls, the resonant frequency, f_c, of the transmission method is always higher than that determined by the cylindrical cavity method. This difference is smaller for samples with higher dielectric constant, and can be further minimized to less than 2% by making the resonator diameter smaller. The accuracy of our transmission method setup has been tested by using two commercially available dielectric resonators: Murata F-series DR[16] and OXIDE barium tetratitanate DR.[17] The results show that the Q-factor agreed to 0.1% of that specified and that f_c was higher by 2 and 0.5% for Murata and OXIDE DRs, respectively. The real part of the dielectric constant, ε', in the X-band was calculated according to:[18]

$$\varepsilon' = \left[\frac{34}{rf_c}\left(\frac{r}{d} + 3.45\right)\right]^2 \quad (2)$$

where r is the radius of DR, d is the thickness of DR, and f_c is the resonant frequency in GHz. Strictly speaking,

Eq.(2) is applicable for $30 < \varepsilon' < 50$, and it underestimates the value of ε' by 5–7% for materials with $20 < \varepsilon' < 30$. Temperature dependence of the resonance frequency was measured in the range of 20–95 °C. For measurement of τ_f, the sample was placed in a porous, low-ε ceramic holder with a small thermal expansion coefficient. The waveguide was wrapped with a resistive heating tape, and the temperature was monitored using a K-type thermocouple attached to the outer surface of the waveguide.

3. Results

The XRD patterns of samples calcined at various temperatures and times are presented in Fig. 1(a) and (b). The phases in each sample identified from JCPDS files are summarized in Table 1. As revealed by XRD analysis, the process of formation of BMT phase is quite different for the two different methods. In method I, single-phase BMT is completely formed only after heating at 1400 °C for 10 h. In contrast, method II yields nearly pure BMT phase after a 2-h treatment at 1000 °C. According to Table 1, the major difference between the two preparation methods is the presence of undesirable intermediate second phases (i.e. $Ba_4Ta_2O_9$, $Ba_5Ta_4O_{15}$) in method I. These phases, being quite stable at 800–1300 °C, impede the formation of single-phase BMT below 1400 °C. Based on our XRD results, formation of BMT in a single-step method can be tentatively described by the following sequence of chemical reactions:

$$x\mathrm{MgO} + x\mathrm{Ta_2O_5} \rightarrow x\mathrm{MgTa_2O_6} \quad (3a)$$

$$x\mathrm{MgTa_2O_6} + 3x\mathrm{BaO} \rightarrow 3x\mathrm{Ba}\left(\mathrm{Mg_{1/3}Ta_{2/3}}\right)\mathrm{O_3} \quad (3b)$$

$$\frac{5}{2}(1-x)\mathrm{BaO} + (1-x)\mathrm{Ta_2O_5} \rightarrow \frac{1}{2}(1-x)\mathrm{Ba_5Ta_4O_{15}} \quad (4a)$$

$$\frac{1}{2}(1-x)\mathrm{BaO} + \frac{1}{6}(1-x)\mathrm{Ba_5Ta_4O_{15}} \rightarrow \frac{1}{3}(1-x)\mathrm{Ba_4Ta_2O_9} \quad (4b)$$

$$\frac{1}{6}(1-x)\mathrm{Ba_5Ta_4O_{15}} + \frac{1}{3}(1-x)\mathrm{Ba_4Ta_2O_9} \rightarrow (1-x)\mathrm{Ba_3Ta_2O_8} \quad (4c)$$

$$(1-x)\mathrm{Ba_3Ta_2O_8} + (1-x)\mathrm{MgO} \rightarrow 3(1-x)\mathrm{Ba}\left(\mathrm{Mg_{1/3}Ta_{2/3}}\right)\mathrm{O_3} \quad (4d)$$

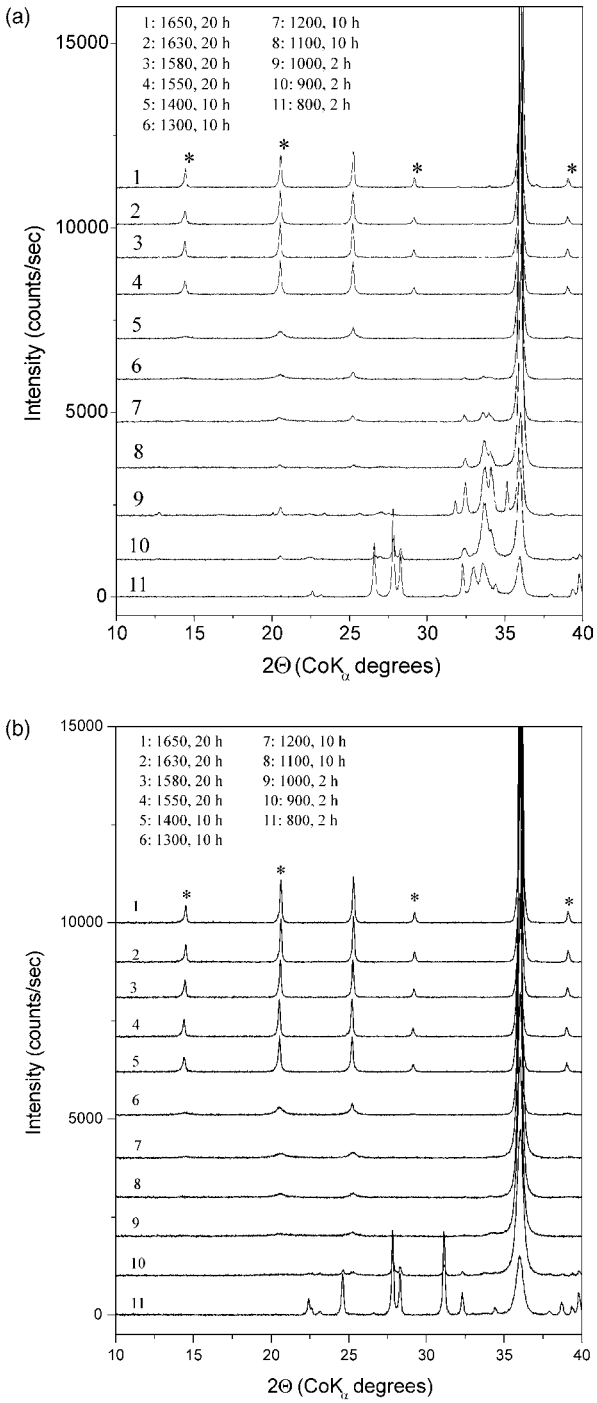

Fig. 1. XRD patterns of method I (a) and method II (b) BMT obtained with CoK_α radiation source ($\lambda = 1.7889$ Å). Superstructure reflections from 1:2 ordered domains are indicated by * symbol.

According to Eqs. (3) and (4), the perovskite phase is formed by at least two different chemical routes due to the possible reactions of Ta_2O_5 with MgO as well as with BaO. In the first case [Eqs. (3)], the perovskite phase forms at temperatures below 1000 °C. However, the amount of the perovskite phase thus formed is small. In the temperature range of 900–1300 °C the two major phases besides BMT are $Ba_4Ta_2O_9$, and

Table 1
Phases comprising BMT samples prepared at different temperatures and soaking

Temperature and soaking time	Method I BMT		Method II BMT	
	Major phases	Minor phases	Major phases	Minor phases
800 °C, 2 h	$BaCO_3$, Ta_2O_5, MgO, $Ba_5Ta_4O_{15}$	$Ba(Mg_{1/3}Ta_{2/3})O_3$	$BaCO_3$, $MgTa_2O_6$, $Ba(Mg_{1/3}Ta_{2/3})O_3$	Ta_2O_5 traces, MgO traces
900 °C, 2 h	$Ba(Mg_{1/3}Ta_{2/3})O_3$, $BaCO_3$, Ta_2O_5, MgO, $Ba_5Ta_4O_{15}$	$Ba_4Ta_2O_9$,	$Ba(Mg_{1/3}Ta_{2/3})O_3$	$BaCO_3$, $MgTa_2O_6$
1000 °C, 2 h	$Ba(Mg_{1/3}Ta_{2/3})O_3$, $Ba_4Ta_2O_9$, $Ba_5Ta_4O_{15}$	Unidentified phase, MgO traces	$Ba(Mg_{1/3}Ta_{2/3})O_3$	
1100 °C, 5 h	$Ba(Mg_{1/3}Ta_{2/3})O_3$, $Ba_5Ta_4O_{15}$	$Ba_4Ta_2O_9$, MgO traces	$Ba(Mg_{1/3}Ta_{2/3})O_3$	
1200 °C, 10 h	$Ba(Mg_{1/3}Ta_{2/3})O_3$	$Ba_4Ta_2O_9$, $Ba_5Ta_4O_{15}$	$Ba(Mg_{1/3}Ta_{2/3})O_3$	
1300 °C, 10 h	$Ba(Mg_{1/3}Ta_{2/3})O_3$	$Ba_4Ta_2O_9$ traces, $Ba_5Ta_4O_{15}$ traces	$Ba(Mg_{1/3}Ta_{2/3})O_3$	
1400 °C, 10 h	$Ba(Mg_{1/3}Ta_{2/3})O_3$		$Ba(Mg_{1/3}Ta_{2/3})O_3$	
1630 °C, 20 h	$Ba(Mg_{1/3}Ta_{2/3})O_3$	$Ba_3Ta_5O_{15}$ traces	$Ba(Mg_{1/3}Ta_{2/3})O_3$	
1650 °C, 20 h	$Ba(Mg_{1/3}Ta_{2/3})O_3$	$Ba_3Ta_5O_{15}$ traces	$Ba(Mg_{1/3}Ta_{2/3})O_3$	$Ba_3Ta_5O_{15}$ traces

$Ba_5Ta_4O_{15}$. One of the mechanisms of their transformation into BMT is described by Eqs. (4c) and (4d). The absence of $Ba_3Ta_2O_8$ in calcined powders suggests that this phase has a labile character (i.e. upon formation it immediately reacts with MgO). An unidentified phase was detected in the powders calcined at 1000 °C. This leads us to conclusion that there exists one more chemical route of formation of BMT besides those described in Eqs. (3) and (4). The powders prepared by method II contained traces of MgO and Ta_2O_5 phases due to incomplete synthesis of $MgTa_2O_6$ precursor. These phases disappeared after heat treatment at 900 °C. No additional second phases were detected during heat treatment of the method II powders. This indicates that the perovskite phase in method II forms directly by reaction of $MgTa_2O_6$ with BaO:

$$3BaO + MgTa_2O_6 \rightarrow 3Ba(Mg_{1/3}Ta_{2/3})O_3 \quad (5)$$

Within the XRD accuracy of 2%, BMT samples obtained by both method I and method II in the temperature range of 1400–1620 °C do not contain any other phases. However, the XRD analysis of method I samples sintered at 1630 and 1650 °C reveals the presence of a small amount of a second phase, identified as $Ba_3Ta_5O_{15}$.[19] Traces of the $Ba_3Ta_5O_{15}$ phase were also detected in the method II BMT sintered at 1650 °C as seen in Fig. 2. It is known that BMT can exist in ordered and disordered forms.[2] In the low-temperature ordered form (space group $P\bar{3}m1$) the Mg^{2+} and Ta^{5+} cations are distributed on individual (111) planes of the perovskite subcell with alternating {Mg, Ta, Ta} layers. This is the 1:2 ordered configuration with the ordered phase having a hexagonal crystal structure. In the high-temperature disordered phase, the Mg^{2+} and Ta^{5+} cations are randomly distributed on octahedral sites of the perovskite subcell which raises the symmetry of the system to cubic (space group *Pm3m*). According to

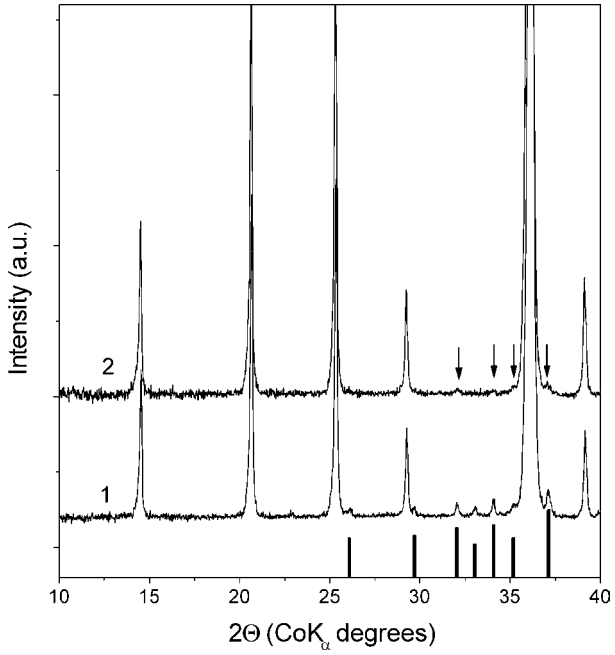

Fig. 2. XRD patterns of method I (1) and method II (2) BMT sintered at 1650 °C for 20 h. Vertical bars represent the relative intensity of reflections from $Ba_3Ta_5O_{15}$ phase. The arrows indicate the traces of $Ba_3Ta_5O_{15}$ phase in method II BMT. CoK_α radiation source ($\lambda = 1.7889$ Å).

Fig. 1, weak reflections from 1:2 ordered BMT domains begin to become visible for powders treated at a temperature as low as 1000 °C. The ordering increases with the annealing temperature. To quantitatively examine the degree of 1:2 ordering in BMT, we determined the ordering parameter, *s*, from[4]

$$s = \sqrt{\frac{\left(I_{100}/I_{110,012}\right)_{obs}}{\left(I_{100}/I_{110,012}\right)_{order}}} \quad (6)$$

where $\left(I_{100}/I_{110,012}\right)_{obs}$ is the ratio of the observed intensity of (100) superstructure reflection to that of

(110) and (012) subcell reflection peaks. The calculated value of $\left(I_{100}/I_{110,012}\right)_{\text{order}}$ for a completely ordered structure is 0.083.[4] The values of the observed intensities, I_{100} and $I_{110,012}$, were found from the area of the corresponding XRD peaks. The ordering parameter, s, for ceramics sintered at different temperatures for 20 h and cooled down to 1400 °C at a rate of 20 °C/h is plotted in Fig. 3. For both methods I and II ceramics the value of s increases with sintering temperature, goes through a maximum of 0.995 at 1580 °C, and then decreases to 0.948 at 1650 °C. To examine the possibility of increasing the degree of ordering by postsinter annealing, ceramics sintered at 1630 and 1650 °C were annealed at 1580 °C for 20 h. However, the value of s did not change.

Fig. 4 shows a bright-field TEM image of BMT sintered at 1580 °C. A selected area electron diffraction (SAD) pattern taken along the [011] main zone axis is shown in insert of Fig. 4. Extra electron diffraction spots at $\{h \pm \frac{1}{3},\ k \pm \frac{1}{3},\ l \pm \frac{1}{3}\}$ from a single 1:2 ordered domain are observed on SAD pattern. It was found that all BMT ceramic samples sintered in the 1570–1650 °C temperature range consist of large (>200 nm) 1:2 ordered domains. However, due to the relatively small electron-transparent area of the samples and large size of the 1:2 domains, it was impossible to perform any statistical analysis of the size of those domains by the electron diffraction technique.

Microstructural observations of the samples revealed a gradual increase of the grain size from 2.5 to 15 μm for ceramics sintered at 1570–1650 °C. The average grain size is listed in Table 2. The second phase was observed on the surface of the thermally etched BMT samples. Fig. 5 shows SEM images of methods I and II BMT samples sintered at 1650 °C and thermally etched at 1450 °C for 2 h. The EDX chemical analysis of the matrix phase and second-phase has revealed that the ratio of the Ba to Ta major peaks equals 0.888 for the matrix and 0.357 for the second-phase. This agrees well with the chemical composition of the second phase of $Ba_3Ta_5O_{15}$. Regarding the formation of this phase the following mechanism is proposed. Owing to the close-packed perovskite structure of BMT and tolerance factor close to unity, it is most likely that Schottky defects predominate in BMT at sintering temperatures. While the equilibrium point defect chemistry of the BMT grain bulk is governed by the mass action relationships, the interfacial concentration of defects is determined by their formation energy. In case of Schottky defects, the interface performs as an ideal source or sink of defects, in other words, defect formation occurs at the interface. The difference in the individual defect formation energies leads to preferential enrichment of the interface in the ion of lower vacancy formation energy. This ion will be predominant in the second phase formed at the interface and in the voids of the matrix grains. Based on our XRD and EDX results, it can be assumed that the Ta ion has the lowest defect formation energy in the BMT compound.

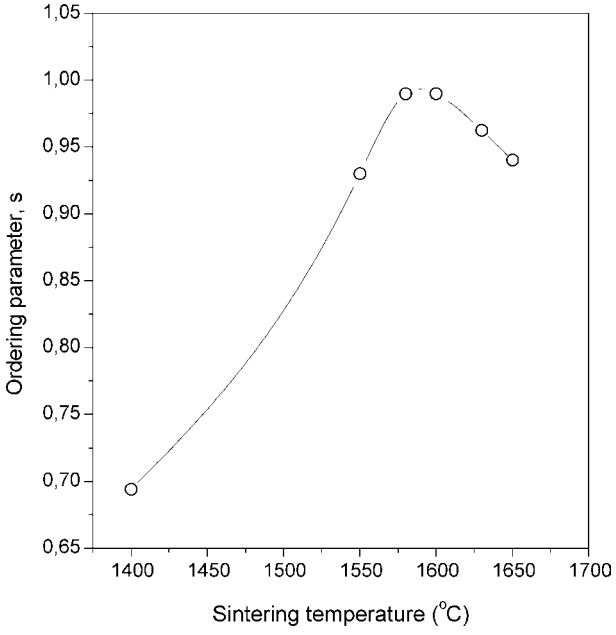

Fig. 3. Dependence of the ordering parameter on the sintering temperature of the method II BMT.

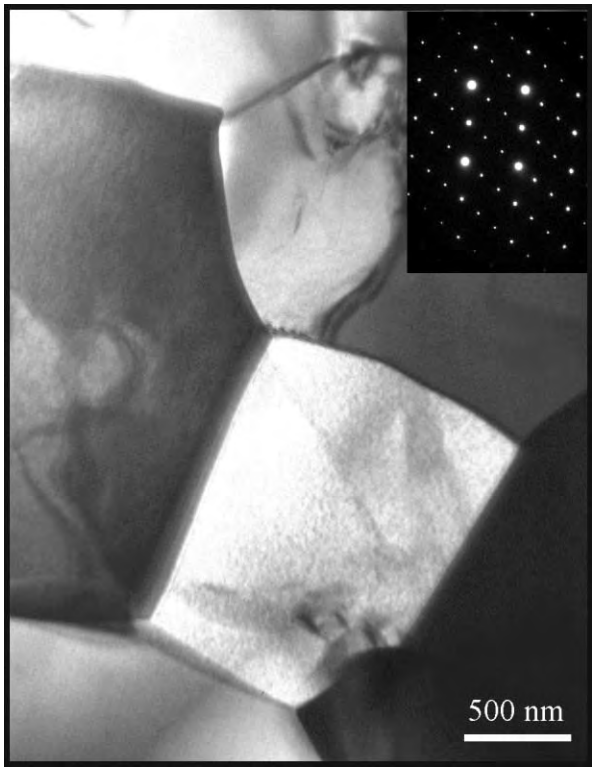

Fig. 4. Bright field TEM image of BMT sample sintered at 1580 °C for 20 h. The insert shows the SAD pattern from a single 1:2 ordered domain.

Table 2
Grain size, τ_f and ε' of BMT ceramics prepared by 2 different methods and sintered at different temperatures for 20 hours

T_{sint},°C	Method I BMT			Method II BMT		
	Grain size, μm	τ_f, ppm/K	ε' at 10 GHz	Grain size, μm	τ_f, ppm/K	ε' at 10 GHz
1580	3.1	0.2	22.0	3.5	−0.3	22.5
1600	5.0	1.8	23.0	6.4	1.2	23.7
1630	15.1	2.9	23.0	14.0	2.5	23.9
1650	20.2	4.1	22.8	21.2	3.5	23.9

Figs. 6 and 7 show the dependence of the relative density and dielectric constant, ε', on sintering temperature. A relative density was calculated from

$$\rho = \frac{\rho_{obs}}{\rho_{th}} \times 100\% \quad (7)$$

where ρ_{obs} is the measured density and $\rho_{th} = 7.657$ g cm^{-3} is the theoretical density of BMT.[20] A meaningful calculation of the density of method I ceramics sintered above 1620 °C was not possible due to the presence of the second phase. However, the microstructural observations of ceramics sintered at 1630 and 1650 °C revealed that method I BMT has a larger proportion of voids than method II ceramics sintered at the same temperatures. We may conclude that over the whole range of sintering temperatures, method II ceramics have a higher density than that of method I. In general, the density of ceramics increases with sintering temperature. Method II ceramic sintered at 1650 °C has the highest density of 97.3%. According to Fig. 7, method II ceramics have higher values of dielectric constant, which can be explained by their higher density. In addition, method I ceramics sintered above 1620 °C show a slight decrease of the dielectric constant with sintering temperature, T_{sint}. The possible reason for such behavior might be the presence of the $Ba_3Ta_5O_{15}$ second phase with apparently low ε'. For method II ceramics, the value of ε' levels off at 24 ± 0.5 for $T_{sint} > 1600$ °C. This value agrees well with the dielectric constant of BMT sintered at 1650 °C reported by Youn et al.[21] We cannot explain anomalously high dielectric constant ($\varepsilon' = 37$) obtained by Tien et al.[22] in BMT

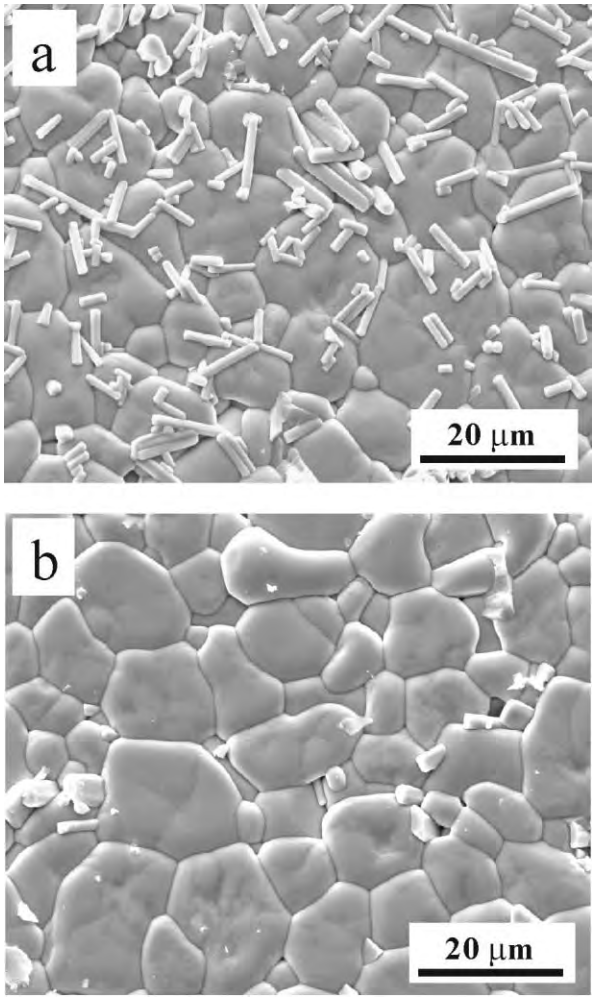

Fig. 5. SEM images of method I (a) and method II (b) BMT sintered at 1650 °C for 20 h.

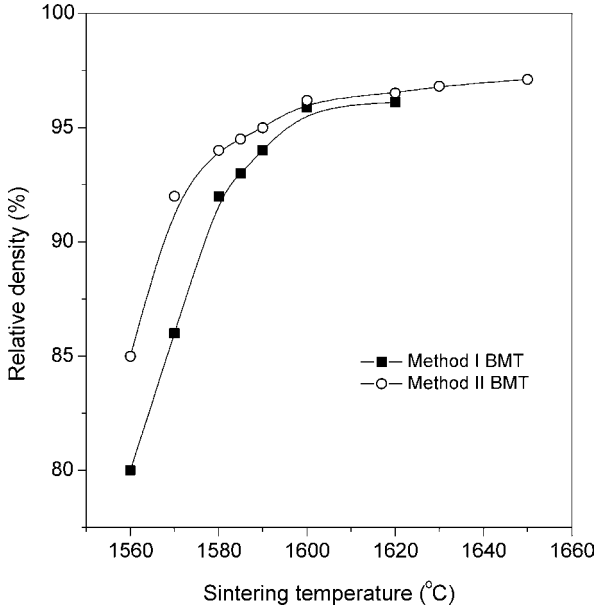

Fig. 6. Dependence of the density of the BMT samples on the sintering temperature. The samples were sintered for 20 h.

sintered at 1600 °C. According to Fig. 8, the dependence of dielectric constant on the porosity of ceramics obeys the Maxwell–Wagner relation[23]

$$\varepsilon' = \varepsilon'_1\left\{1 + \frac{3\gamma(\varepsilon'_2 - \varepsilon'_1)}{2\varepsilon'_1 + \varepsilon'_2}\right\} \quad (8)$$

where $\varepsilon'_1 = 25$ for completely dense BMT ceramics, ε'_2 is the permittivity of vacuum, and γ is the porosity of ceramics.

Fig. 9 shows the dependence of $Q \times f$ (hereafter referred to as the efficacy factor, $F = Q \times f$) on sintering temperature with the bars showing the range of variation of F. The curves show a maximum at $T_{sint} = 1590$ °C for method I BMT and at $T_{sint} = 1580$ °C for method II BMT. As also evident from Fig. 9, the maximum values of F obtained for method I and II ceramics were 200 and 280 THz, respectively. The value of F decreases appreciably for samples sintered both above and below 1585 ± 5 °C. It is worth noting that the density of ceramics exhibiting the highest value of F was approximately 94%. For samples sintered below 1580 °C, the low value of F can be attributed both to poor densification and insufficient ordering in B-sublattice. For samples sintered above 1590 °C, although the density continues to increase, F decreases and reaches a value of 80–130 THz at $T_{sint} = 1650$ °C.

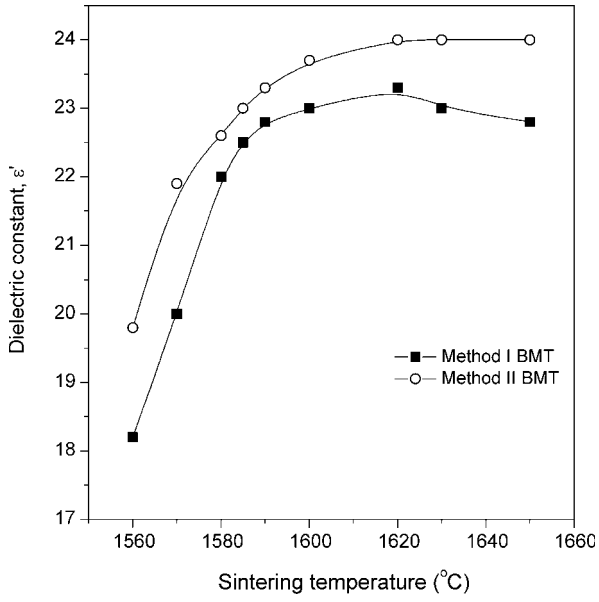

Fig. 7. Dependence of the dielectric permittivity at 10 GHz on sintering temperature for BMT sintered for 20 h.

Measurement of the temperature coefficient of the resonant frequency, τ_f, of BMT DRs, which was performed by using a rectangular copper waveguide, gives a total temperature coefficient of the resonance frequency, τ_f^t, of the whole *waveguide* and *DR* system by the equation:

$$\tau_f^t = \tau_f^w + \tau_f \quad (9)$$

where $\tau_f^w$is a temperature coefficient of the resonance frequency of the waveguide, and τ_f is the temperature coefficient of the resonance frequency of the DR without enclosure. According to O'Bryan,[24] τ_f is given by

$$\tau_f = -\alpha - \frac{1}{2}\tau_\varepsilon \quad (10)$$

where α is the linear thermal expansion coefficient of the DR ($\alpha = \frac{d\ln l}{dT}$), and τ_ε is the temperature coefficient of the

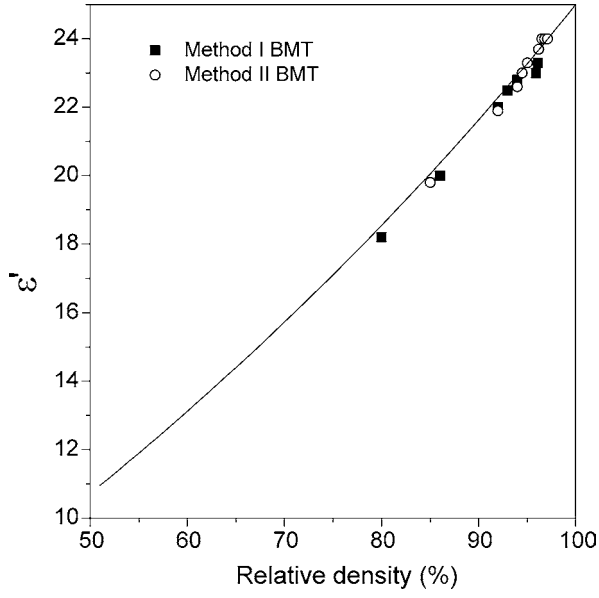

Fig. 8. Dependence of the dielectric constant on the density of BMT samples. The solid line was calculated from Eq. (8).

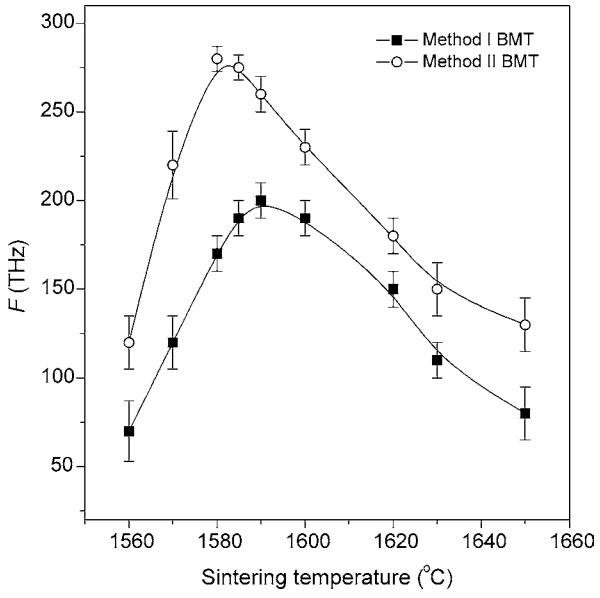

Fig. 9. Dependence of the efficacy factor F on the sintering temperature of BMT samples. The samples were sintered for 20 h.

dielectric constant. The value of τ_f^w is specific to the thermal expansion coefficient of the waveguide material and to the spacing between the waveguide walls and the DR, which makes its accurate determination difficult. In order to obtain an approximate value of τ_f in Eq. (9), we calculated the value of τ_f^w by using a similar size dielectric resonator with known τ_f.[16] It was found that our copper waveguide had $\tau_f^w \approx -1.2 \pm 0.5$ ppm/K. The shift of the resonant frequency, Δf_c, of the whole *waveguide* and *DR* system with increase in temperature is shown in Fig. 10. The values of τ_f for BMT ceramics sintered at different temperatures were determined from Eq. (10) and are listed in Table 2. Both the data in Table 2 and curves in Fig. 10 show that τ_f increases with sintering temperature.

4. Discussion

Since ε' the BMT crystal is entirely determined by the polar phonon contribution, no dielectric dispersion is expected below the submillimeter range. The behavior of ε'', however, is more complex. According to Tagantsev et al.,[25] two frequency regimes of ε'' variation should be distinguished: (i) at frequencies between γ_T and Ω_i where Ω_i is the eigenfrequency of the i-th phonon mode, and γ_T is the averaged damping of thermally populated phonons, the frequency dependence of ε'' is given by $\varepsilon''(\omega) \propto T\omega^2$, (ii) at ω below γ_T, ε'' is linearly proportional to frequency, i.e. $\varepsilon''(\omega) \propto T^2\omega$. In the microwave range, the energy of photons is much lower than that of optical phonons. Thus, due to the energy conservation requirements, the incident photons cannot be absorbed by the excitation of the transverse optical (TO) phonons. Hence, at temperatures of the order of the Debye temperature or higher, the major dielectric loss comes from the two-phonon difference absorption[26] (three-quantum process). In this process, an incident photon couples to an intermediate TO phonon which in turn couples to two other phonons. One phonon is absorbed and another created with the energy difference being equal to the energy of the incident photon. Due to the small energy of the incident photon in the microwave range, this process occurs close to the lines of degeneracy of the phonon branches in the Brillouin zone. High-temperature order–disorder transition of BMT from low to high crystal symmetry increases the number of degeneracies of the phonon modes. This in turn will increase the dielectric loss due to the increased probability of the three-quantum process. Our experimental results presented in Figs. 3 and 9 clearly confirm this assumption. The decrease of the F follows the decrease of the ordering parameter, s, for samples sintered above 1590 °C.

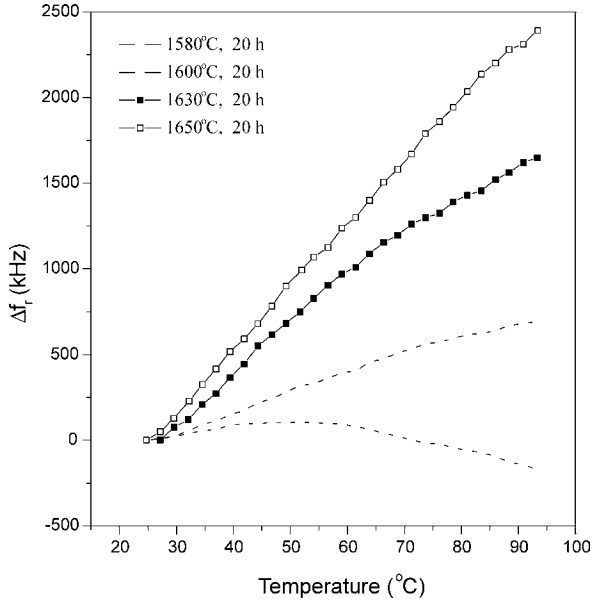

Fig. 10. Temperature dependence of the shift of the resonance frequency of method I BMT dielectric resonators sintered at different temperatures.

In addition to purely intrinsic dielectric loss, extrinsic loss due to defects, impurities, porosity, second phase, and grain boundaries will also contribute to the lowering of the Q-factor. It is found that ceramics prepared by method I have higher porosity and lower F compared with method II BMT. The $Ba_3Ta_5O_{15}$ second phase is found by EDX and XRD in BMT sintered above 1630 °C. The second phase was mostly concentrated on the internal surface of the voids. Formation of Ta-rich second phase will change the stoichiometric composition of BMT grains by introducing tantalum vacancies into BMT matrix. Since the process of disordering involves interdiffusion of B' and B'' cations it will be significantly facilitated in the region of high vacancy concentration.

As mentioned above, our experimental results have shown that the degree of 1:2 ordering in BMT starts to decrease for samples sintered above 1585 ± 5 °C. This temperature, however, is much lower than that obtained in the theoretical work of Takahashi et al.[9] We suggest that this difference may originate from the fact that in the cluster calculations of Takahashi et al.[9] vacancies were not taken into account. We believe that the presence of vacancies in the BMT structure at sintering temperatures will significantly lower the temperature of the order–disorder phase transition. Similar arguments were proposed by Hong et al.[27] who studied the order–disorder transition in $Ba(Ni_{1/3}Nb_{2/3})O_3$ and $Ba(Zn_{1/3}Nb_{2/3})O_3$. They reported formation of appreciable amounts of a Nb-rich liquid phase in samples sintered near and above the order–disorder phase transition (T_c = 1300–1350 °C). The temperature of order–disorder phase transition in $Ba(Zn_{1/3}Nb_{2/3})O_3$ was found to be also much lower than that calculated by Takahashi et al.[9] We found that neither slow cooling nor postsinter

annealing at 1580 °C for 20 h could reinstate the high degree of ordering in BMT ceramics sintered at 1630 and 1650 °C. This suggests that upon cooling from sintering temperature, the high-temperature disordered phase in BMT becomes thermoelastically arrested. Thus, in order to obtain low-loss BMT ceramics, it is crucial to preserve a high degree of B-site cation ordering starting from the earliest stages of sintering. This can be done by both reducing the sintering temperature at the expense of sintering time and by reducing the heating rate to avoid a fast mass transport during nucleation and growth of the 1:2 ordered phase.

5. Conclusions

As revealed by XRD and microwave dielectric measurements, the highest degree of B-site cation ordering in BMT was achieved for samples sintered at $T_{sint} = 1585 \pm 5$ °C. For samples sintered above this temperature, the high degree of ordering cannot be recovered by prolonged postsinter annealing or by slow cooling. Therefore, we conclude that the high temperature order–disorder transition in BMT is an elastic energy arrested first-order phase transition. Another finding of this work is that the synthesis of BMT ceramics by method II from $MgTa_2O_6$ precursor results in a higher ceramic density and superior dielectric properties over the traditional mixed oxide method.

Acknowledgements

The authors acknowledge Dr. M. You, A. Zybura and W. Fitzpatric from ComDev Corp. for their interest and support of this work, and Dr. Yanchevsky and Dr. J. Barbier for useful discussions. T.V.K. acknowledges NSERC for financial support.

References

1. Klein, N., Scholen, A., Tellmann, N., Zuccaro, C. and Urban, K. W., Properties and applications of HTS-shielded dielectric resonators: a state-of-the-art report. *IEEE Transactions on Microwave Theory and Techniques*, 1996, **44**, 1369–1373.
2. Guo, R., Bhalla, A. S. and Cross, L. E., $Ba(Mg_{1/3}Ta_{2/3})O_3$ single crystal fiber grown by the laser heated pedestal growth technique. *J. Appl. Phys*., 1994, **75**, 4704–4708.
3. Nomura, S., Toyama, K. and Kaneta, K., $Ba(Mg_{1/3}Ta_{2/3})O_3$ ceramics with temperature-stable high dielectric constant and low microwave loss. *Jpn. J. Appl. Phys*., 1982, **21**, L624–L626.
4. Matsumoto, K., Hiuga, T., Takada, K. and Ichimura, H., $Ba(Mg_{1/3}Ta_{2/3})O_3$ Ceramics with ultra-low loss at microwave frequencies. In *Proceedings of the 6th IEEE International Symposium on Applications of Ferroelectrics*, 1986, pp. 118–121.
5. Matsumoto, H., Tamura, H. and Wakino, K., $Ba(Mg,Ta)O_3$–$BaSnO_3$ high-Q dielectric resonator. *Jpn. J. Appl. Phys*., 1991, **30**, 2347–2349.
6. Furuya, M. and Ochi, A., Microwave dielectric properties for $Ba(Mg_{1/3}Ta_{2/3})O_3$–$A(Mg_{1/2}W_{1/2})O_3$ (A = Ba, Sr, and Ca) ceramics. *Jpn. J. Appl. Phys*., 1994, **33**, 5482–5487.
7. Burton, B. P., Empirical cluster expansion models of cation order–disorder in $A(B'_{1/3}B''_{2/3}(O_3)$ perovskites. *Phys. Rev. B*, 1999, **59**, 6087–6091.
8. Burton, B. P. and Cockayne, E., Why $Pb(B,B')O_3$ perovskites disorder at lower temperatures than $Ba(B,B')O_3$ Perovskites. *Phys. Rev. B*, 1999, **60**, R12542–R12545.
9. Takahashi, T., Wu, E. J., Van Der Ven, A. and Ceder, G., First-principles investigation of B-site ordering in $Ba(Mg_xTa_{x-1})O_3$ microwave dielectrics with the complex perovskite structure. *Jpn. J. Appl. Phys*., 2000, **39**, 1241–1248.
10. Chai, L., Akbas, M. A., Davies, P. K. and Parise, J. B., Cation ordering transformations in $Ba(Mg_{1/3}Ta_{2/3})O_3$-$BaZrO_3$ perovskite solid solutions. *Mater. Res. Bull*., 1997, **32**, 1261–1269.
11. Swartz, S. L. and Shrout, T. R., Fabrication of perovskite lead magnesium niobate. *Mater. Res. Bull*., 1982, **17**, 1245–1250.
12. Yanchevsky, O.Z., Synthesis and properties of niobium and tantalum complex oxides with perovskite-type structure. PhD thesis, Institute of General and Inorganic Chemistry, Kyiv, Ukraine, 1996.
13. Zurmühlen, R., Petzelt, J., Kamba, S., Kozlov, G., Volkov, A., Gorshunov, B., Dube, D., Tagantsev, A. and Setter, N., Dielectric spectroscopy of $Ba(B'_{1/2}B''_{1/2})O_3$ complex perovskite ceramics: correlations between ionic parameters and microwave dielectric properties. II. Studies below the phonon eigenfrequencies (10^2–10^{12} Hz). *J. Appl. Phys*., 1995, **77**, 5351–5364.
14. Bokrinskaya, A.A., Ilchenko, M.E., Dielectric MW resonator in the transmission line. *Izvestiya Vuzov SSSR, Ser. Radioelectronika*, 1971, XIV (2), 151 (in Russian).
15. *Dielectric Resonators and Related Products: A Designer's Guide to Microwave Dielectric Ceramics*. Trans-Tech, 1996.
16. Murata DRD065FD029A, $Q = 30{,}000$, $f_c = 9.98$ GHz, $\varepsilon = 24 \pm 1$, $\tau_f = 2 \pm 1$ ppm/°C.
17. OXIDE, $BaTi_4O_9$, $Q = 6000$, $f_c = 9.6$ GHz, $\varepsilon = 36 \pm 0.5$, $\tau_f = 0 \pm 0.3$ ppm/°C.
18. Kajfez, D. and Guillon, P. ed., *Dielectric Resonators*. Artech Hause, Inc, 1986, p. 3.
19. Powder Diffraction File, # 83-0713.
20. Galasso, F. S., *Structure, Properties and Preparation of Perovskite-type Compounds*. Pergamon Press, Oxford, 1969.
21. Youn, H-J., Kim, K-Y. and Kim, H., Microstructural characteristics of $Ba(Mg_{1/3}Ta_{2/3})O_3$ ceramics and its related microwave dielectric properties. *Jpn. J. Appl. Phys*., 1996, **35**, 3947–3953.
22. Tien, L.-C., Chou, C.-C. and Tsai, D.-S., Microstructure of $Ba(Mg_{1/3}Ta_{2/3})O_3$-$BaSnO_3$ microwave dielectrics. *Ceram. International*, 2000, **26**, 57–62.
23. Hill, N. E., Vaughan, W. E., Price, A. H. and Davies, M., *Dielectric Properties and Molecular Behaviour*. Van Nostrand Reinhold Company, London, 1969 p. 283.
24. O'Bryan, H. M., Thomson, J. and Plourde, J. K., A new BaO-TiO_2 compound with temperature-stable high permittivity and low microwave loss. *J. Am. Ceram. Soc*., 1974, **57**, 450–453.
25. Tagantsev, A. K., Petzelt, J. and Setter, N., Relation between intrinsic microwave and submillimeter losses and permittivity in dielectrics. *Solid State Comm*., 1993, **87**, 1117–1120.
26. Gurevich, V. L. and Tagantsev, A. K., Intrinsic dielectric loss in crystals. *Adv. Phys*., 1991, **40**, 719–767.
27. Hong, K. S., Kim, I.-T. and Kim, C.-D., Order–disorder phase formation in the complex perovskite compounds $Ba(Ni_{1/3}Nb_{2/3})O_3$ and $Ba(Zn_{1/3}Nb_{2/3})O_3$. *J. Am. Ceram. Soc*., 1996, **79**, 3218–3224.